

Correlation between giant magnetoresistance and magnetic interactions in a CoAg multilayered/granular system

A. D. C. Viegas, J. Geshev, L. F. Schelp, and J. E. Schmidt

Citation: [Journal of Applied Physics](#) **82**, 2466 (1997); doi: 10.1063/1.366058

View online: <http://dx.doi.org/10.1063/1.366058>

View Table of Contents: <http://scitation.aip.org/content/aip/journal/jap/82/5?ver=pdfcov>

Published by the [AIP Publishing](#)



Re-register for Table of Content Alerts

Create a profile.



Sign up today!



Correlation between giant magnetoresistance and magnetic interactions in a CoAg multilayered/granular system

A. D. C. Viegas,^{a)} J. Geshev, L. F. Schelp, and J. E. Schmidt
*Instituto de Física, Universidade Federal do Rio Grande do Sul, C.P. 15051,
91501-970 Porto Alegre, RS, Brazil*

(Received 17 December 1996; accepted for publication 7 May 1997)

Magnetizing, demagnetizing, and remanent magnetization curves for $[\text{Co}(12 \text{ \AA})/\text{Ag}(60 \text{ \AA})] \times 15$ multilayered/granular films thermally treated have been measured. The changes of the giant magnetoresistance and the interaction effects have been explained as a result of the structural, morphological, and magnetic evolution of the samples as a function of the thermal treatment. It has been inferred that for samples annealed at temperatures lower than 360 °C, the changes of the giant magnetoresistance come from the misalignment of the magnetic moments of the Co particles formed during annealing. A strong correlation between the giant magnetoresistance and the magnetic interaction effects has been found for samples annealed at temperatures higher than 360 °C: the giant magnetoresistance is degraded as the demagnetizing interparticle interactions are increased.

© 1997 American Institute of Physics. [S0021-8979(97)01016-5]

I. INTRODUCTION

Since its discovery in magnetic multilayers,¹ giant magnetoresistance (GMR) has been observed in several different kinds of systems including granular systems^{2,3} and multilayers composed of immiscible elements submitted to proper annealing treatment. As first demonstrated for Co/Ag,^{4,5} the thermally treated multilayers represent an intermediate state between multilayer and granular structures, as the as-made samples are progressively modified by the annealing.

Although the GMR in the thermally treated multilayered systems is no greater than 6% at room temperature (about 20% at 4 K), they have received attention for its sensitivity at low fields when soft magnetic material is used.⁶ However, the origin of this effect and its relation to the structural properties (interface roughness, particle shape and size, intergranular distances, etc.) is still a source of controversy.

For instance, Hylton *et al.*⁶ proposed that the appearance of GMR is concurrent with the breakup of the layers, which is attributed to a magnetic interaction that favors local antiparallel alignment of the magnetizations in adjacent layers. The plateletlike grains stack in a columnar structure through the magnetic layers.

Alternatively, the appearance of GMR in the same systems can also be explained using the model applied successfully for the granular systems: the annealing destroys the multilayer structure producing grains with different sizes and shapes, and the GMR arises from the random orientations of the easy magnetization directions. Here, no coupling among the magnetic entities is necessary to explain the appearance of the GMR; spin dependent scattering originates from randomly aligned single domain regions.

In order to achieve some insight into what mechanism is actually present or which one is predominant when both act simultaneously, we studied the magnetic interaction effects (and its correlation to GMR) in Co/Ag multilayered films submitted to thermal annealing.

For granular system, assuming that the particles are superparamagnetic ones, a parabolic behavior of the fractional magnetoresistance as a function of the reduced magnetization M/M_s is expected.³ However, significant deviations from the parabolic law have been observed in different real systems,⁷⁻⁹ indicating correlation between the magnetic moments. Recently, an analytical theory which takes explicitly into account this correlation was proposed by Allia *et al.*¹⁰ in order to explain the observed flattening of the GMR vs M/M_s curve at low fields.

The presence of correlation between the magnetic precipitates has been observed by means of independent magnetic measurements^{11,12} and even direct observation of the formation of domain structures using electron microscopy with polarization analysis.¹³

For most of our samples, the coercive field values from the magnetization curves do not coincide with the fields of the maxima in the magnetoresistance curves, indicating that there is more than one magnetic phase contributing to the magnetization. This does not allow the use of the above deviation to estimate the interparticle interaction strength, as this quadratic law is valid for systems of superparamagnetic particles only.

Recently, the δM plot¹⁴ technique was used to investigate the same effects in Fe/Cu multilayers¹⁵ and $\text{Co}_{10}\text{Cu}_{90}$ granular alloys.¹⁶ This plot appeared to be very sensitive to small changes in the remanence produced by interactions between the magnetic entities.

Nonuniaxial or manyfold planar anisotropies sometimes are present in multilayers. To avoid the introduction of errors induced by any of these anisotropies in our analysis, we measured the magnetization curves applying the magnetic field in different in-plane directions for each sample. As it is not possible to repeat a measurement of the conventional δM plot (starting from ac or the thermal demagnetization state) on the same piece of a sample, we introduce a new interaction plot which permits this to be done. The definition of the new plot is described in Sec. II.

^{a)}Electronic mail: dcveigas@if.ufrgs.br

II. DEFINITION OF THE INTERACTION PLOT

The estimation of the magnetic interaction effects in particulate and thin film media in the recent years is based on the Wohlfarth relation¹⁷ $M_d(H) = 1 - 2M_r(H)$, where $M_r(H)$ and $M_d(H)$ are the reduced remanent magnetizations [normalized by saturation remanence $M_r(\infty)$], and H is the external field. The $M_r(H)$ curve is obtained after application and removal of the field H to the demagnetized state, and the $M_d(H)$ curve is obtained after application and removal of the field $-H$ to the saturation remanence. Plots of $M_d(H)$ vs $M_r(H)$ have come to be known as Henkel plots.¹⁸ For uniaxial anisotropy particles the noninteracting case corresponds to a linear plot with a gradient -2 . Positive values of δM plot, defined by Kelly *et al.*¹⁴ as $\delta M(H) = M_d(H) - 1 + 2M_r(H)$, were attributed to “magnetizing” interactions, i.e., interactions promoting the magnetized state while negative values were related to “demagnetizing” interactions, which tend to assist magnetization reversal. This relationship is also valid for multi-domain ferromagnets if the walls interact with the same density and distribution of pinning sites on both the initial and demagnetization branches of the magnetization curve.¹⁹

The $M_r(H)$ curve depends on the method by which the demagnetized state is produced, and dc, ac, or thermal demagnetization give very different initial remanent magnetization curves (see, for example, Ref. 20).

Bissel *et al.*²¹ derived a connection between the isothermal remanent magnetization curve after dc demagnetization, M_r^{dc} , and $M_d(H)$. The M_r^{dc} curve is produced by cycling the sample to the negative remanence coercivity ($-H_r$) after previous saturation and then reducing the applied field to zero. After dc demagnetization the particles with switching fields $< H_r$ are reversed while those requiring fields $\geq H_r$ remain magnetized in the direction of the original saturation remanence. The resulting connections are:

$$M_r^{dc}(H) = 1 - M_d(H), \quad (1)$$

for $H < H_r$, and

$$M_r^{dc}(H) = 1 \quad (2)$$

for $H \geq H_r$.

Here we used a new, $\delta M^{dc}(H)$ plot, recently introduced by Viegas *et al.*¹⁶ as

$$\delta M^{dc}(H) = M_r^{dc}(H) - 1 + M_d(H). \quad (3)$$

for $H < H_r$, and

$$\delta M^{dc}(H) = M_r^{dc}(H) - 1 \quad (4)$$

for $H \geq H_r$.

In the case of no interaction (and uniaxial anisotropy) $\delta M^{dc}(H)$ is zero for all values of H .

III. EXPERIMENT

Two multilayered samples deposited on a Si (111) substrate by means of electron beam guns have been investigated. The first one has nominal $[\text{Co}(12 \text{ \AA})/\text{Ag}(60 \text{ \AA})] \times 15$ evaporated over a 50 \AA Cr buffer layer first; and the other sample is the same but has no Cr buffer layer. The thermal

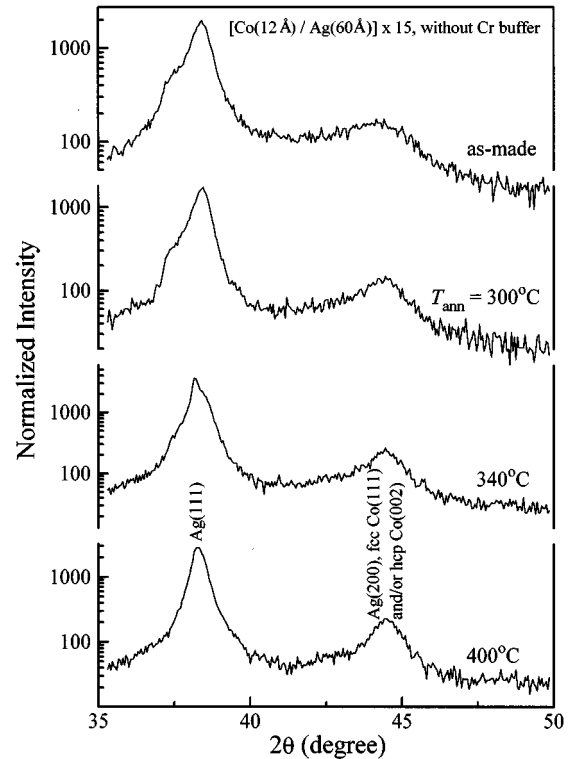


FIG. 1. High angle x-ray diffraction patterns for the as-made $[\text{Co}(12 \text{ \AA})/\text{Ag}(60 \text{ \AA})] \times 15$ multilayer sample without Cr buffer; similar results are obtained for the other sample.

treatment was performed in a rapid annealing furnace under argon atmosphere between $150 \text{ }^\circ\text{C}$ and $450 \text{ }^\circ\text{C}$ for 1 h.

The $\theta : 2\theta$ x-ray diffractometry was used to check the structural properties of the samples (high angle diffraction patterns are displayed in Fig. 1). The broad peaks observed at low and high angles indicate a polycrystalline multilayered structure with (111) textured Ag layers: with the arrangement used we cannot obtain information about the Co structure. From the full width at half height of the peaks, the perpendicular coherence length was estimated to be slightly greater than the period of the multilayers, indicating fluctuations in the thickness throughout the samples.

The magnetoresistance was measured in fields up to 8.5 kOe using the standard four-probe method. Magnetization measurements were performed at room temperature using an alternating gradient magnetometer (AGM) with the field applied parallel to the plane of the sample. The initial magnetization curves, hysteresis loops, as well as remanent magnetization curves were measured. By changing the in-plane applied field direction, no significant changes in all of the curves were observed for the sample with Cr buffer. Figure 2(a) shows the isothermal remanent magnetization curve after dc demagnetization, $M_r^{dc}(H)$, dc demagnetization remanence curve, $M_d(H)$, as well as the here defined $\delta M^{dc}(H)$ plots for this sample annealed at $150 \text{ }^\circ\text{C}$.

The samples without Cr buffer layer and annealed up to $300 \text{ }^\circ\text{C}$ showed in-plane magnetic anisotropy, and the ones annealed at higher temperatures were magnetically isotropic.

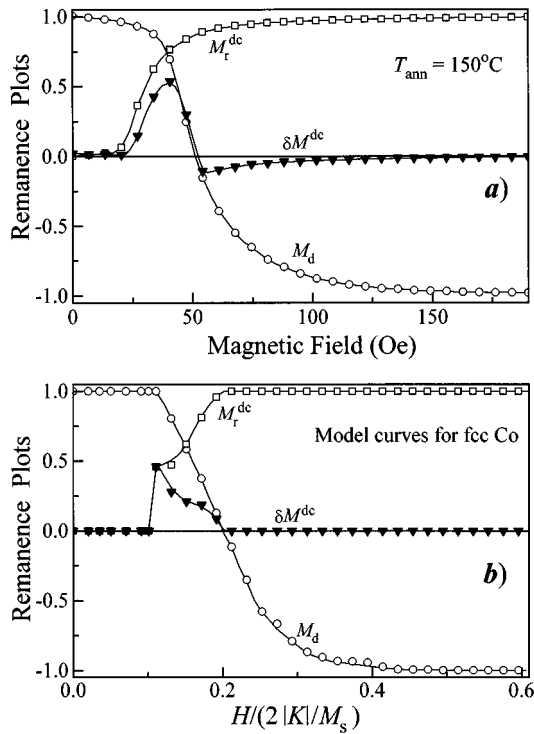


FIG. 2. (a) Representative remanence curves $M_r^{\text{dc}}(H)$, $M_d(H)$ and the here defined $\delta M^{\text{dc}}(H)$ plot for the sample with Cr buffer annealed at 150°C . (b) Model $\delta M^{\text{dc}}(H)$ plot for a disordered system of noninteracting cubic anisotropy particles ($K < 0$).

IV. RESULTS AND DISCUSSION

For all of the samples, the δM^{dc} plots are characterized by a large positive peak in lower fields and a relatively shallow minimum in higher fields.

From the large reduced saturation remanence $M_r(\infty)$ and the positive δM^{dc} plots for the as-made samples and the ones annealed at temperatures lower than 300°C , one can suggest that there is only fcc Co in the samples and weak interactions present. This suggestion is supported by:

- (i) the theoretical $M_r(\infty) = 0.866^{22}$ is very close to our data, and
- (ii) the δM^{dc} plot for a disordered system of noninteracting cubic anisotropy particles with four easy magnetization axes calculated here following the model of Geshev and Mikhov²³ and Eqs. (3) and (4) [Fig. 2(b)], has shape similar to that of the experimental plots, and even the value of the maximum is almost the same.

(Here K is the first cubic anisotropy constant, which is negative for fcc Co.)

An alternative suggestion can be a relatively strong intralayer coupling between the adjacent magnetic regions, and coexistence of fcc and uniaxial hcp Co. For many uniaxial magnetic materials, such a behavior is attributed to strong exchange interactions between the adjacent layers or grains.²⁴ These interactions initially stabilize the magnetized state followed by rapid cooperative switching of many magnetic moments above a critical field. A similar interaction

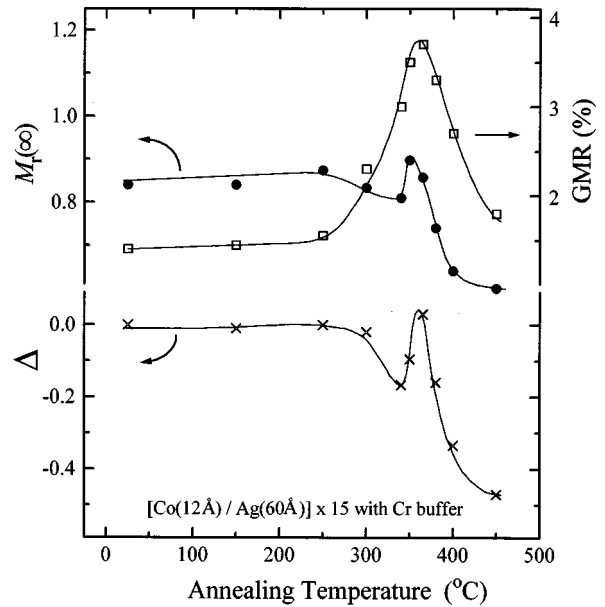


FIG. 3. GMR, Δ [defined as $\Delta = \delta M_{\text{max}}^{\text{dc}}(T_{\text{ann}}) - \delta M_{\text{max}}^{\text{dc}}(\text{as-made})$] and the reduced saturation remanence $M_r(\infty)$ as a function of the annealing temperature for $[\text{Co}(12 \text{ \AA})/\text{Ag}(60 \text{ \AA})] \times 15$ multilayer evaporated over a 50 \AA Cr buffer layer. The solid lines are guide to the eye.

behavior has been observed for many magnetic systems, such as thin films of CoP,¹⁴ CoNiCr,^{24,25} CoCrTa,²⁵ CoSm/FeCo,²⁶ and other double and triple magnetic layered media.²⁷ For the case of the Co/Ag system, due to the rather thick (60 \AA) Ag spacer, interlayer interactions are weak and cannot be responsible for the large reduced remanence: as was shown by van Alphen and de Jonge,²⁸ the remanent magnetization of multilayers of Co/Ag composition with continuous Co layers is independent of the Ag layer thickness. The same authors showed coexistence of both fcc and hcp Co phases from ^{59}Co nuclear magnetic resonance experiments in Co/Ag multilayers.

To estimate the change of the strength of the interactions as a function of the annealing temperature T_{ann} , we used the relative maxima of the δM^{dc} plots, i.e., $\Delta = \delta M_{\text{max}}^{\text{dc}}(T_{\text{ann}}) - \delta M_{\text{max}}^{\text{dc}}(\text{as-made})$. Any change of the Δ is attributed to change of the relative strength of the interactions, which may be both exchange and dipolar in nature, leading to complex magnetic behavior.

The reduced remanence $M_r(\infty)$, reduced GMR ratio, defined as $[R(H_c) - R(H_{\text{max}})]/R(H_c)$ (where R is the resistance, H_c is the coercive field and H_{max} is the maximum applied field), and Δ versus the annealing temperature for the sample with Cr buffer are plotted in Fig. 3. There is a relatively sharp peak in the GMR at about 360°C , in accordance with the previous published results.^{4,5,29} Δ and $M_r(\infty)$ show minima at 340°C , followed by sharp maxima at the same annealing temperature where GMR is maximum.

Figure 4 displays the dependencies of the coercivity factor (CF),³⁰ defined as $\text{CF} = (H_r - H_c)/H_c$ on T_{ann} for the same sample [here H_r is the remanence coercivity, i.e., $M_d(H_r) = 0$]. The dotted and the dashed lines represent the noninteracting cases for fine particle systems with uniaxial ($\text{CF} \approx 9\%$)³⁰ and cubic anisotropy ($\text{CF} \approx 4\%$),²³ respec-

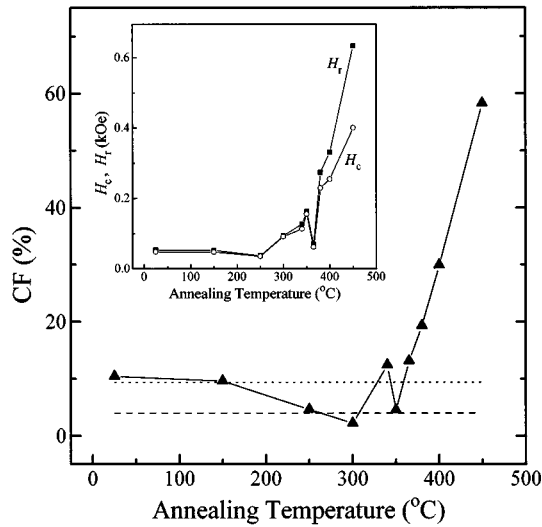


FIG. 4. Coercivity factor (CF) defined as $CF = (H_r - H_c)/H_c$ on T_{ann} for the sample evaporated over a Cr buffer layer; the dotted and the dashed lines represent the noninteracting cases for the uniaxial and cubic anisotropy case, respectively; the inset shows the corresponding $H_c(T_{ann})$ and $H_r(T_{ann})$ plots.

tively. The inset in this figure shows the corresponding $H_c(T_{ann})$ and $H_r(T_{ann})$ plots. A general trend of increase is observed in both curves, except for the $T_{ann} = 360^\circ\text{C}$, where lower values are obtained. A slight decrease of CF is observed for annealing up to 300°C . Thermal treatment at a temperature higher than 350°C leads to a roughly linear rapid increase of CF.

The data from this figure support the suggestion that for T_{ann} up to 360°C the interactions are weak: the CF values lay (with small deviations) in the range between the dotted and dashed lines, representing the noninteracting uniaxial and cubic anisotropy cases. That is exactly where CF data should be placed if one has a sample, which is a mixture of fcc and hcp Co.

The correlation between GMR and the variations of the magnetic interactions is discussed below, based on these data and on the structural, morphological, and magnetic evolution of the samples due to annealing.

For annealing up to 300°C there are no significant changes in the physical parameters of Figs. 3 and 4. Treatment at temperatures lower than 300°C does not lead to appreciable structural changes of the samples as well (Fig. 1). Having Co and Ag immiscible over a large temperature range, one first induces a back-diffusion process upon annealing at low temperatures, thus effectively obtaining smoother interfaces,⁴ but the overall magnetic characteristics of the sample remain the same.

For annealing at higher temperatures gradual destruction of the multilayers and formation of granular Co begins. Initially, the multilayers break up into rather bulky ‘‘pancake-like’’ clusters.²⁸ Such a transition from continuous to discontinuous magnetic layers upon annealing is found in a number of Co/Ag multilayers.^{4,5,29}

The nonmagnetic Ag matrix between the Co clusters is metallic, and hence, can support Ruderman-Kittel-Kasuya-Yosida (RKKY) interactions which might be expected to

couple the adjacent magnetic regions of appropriate geometry. However, it was recently shown³¹ that beyond a certain critical cluster size, the coupling is entirely dominated by the dipolar term. Such interactions could be either magnetizing or demagnetizing depending on the interparticle distance and configuration. In the present case, the majority of the Co grains within the Co layers are supposed to be weakly coupled. Further annealing results in a transition of the shape of the clusters from flat pancake to more spherical shaped and, in general, in a decrease of their size, as well as a decrease of the lateral distances between the clusters. As a result, the local interparticle interactions can change their strength and even the sign during annealing, thus leading to the singularities in the $M_r(\infty)$, Δ , H_c , H_r , and CF plots versus the annealing temperature up to 360°C .

Annealing at temperatures higher than 300°C leads to a relatively sharp increase of the GMR. This increase could be explained in the framework of the model of Xiao *et al.*³ without the intricate antiferromagnetic coupling, assuming that the main contribution to the GMR comes from the random orientation of the magnetic moments: the annealing destroys the layered structure, changing the Co particle number and sizes. Initially, the Co particles are few in number. Scattering effects are infrequent and far apart, resulting in small GMR. Further annealing increases the number of the particles, decreases their sizes, and changes the distance between them, which approximate to their optima (for the magneto-resistance) values: the magnitude of GMR is thus enhanced.

Having reached maxima at $T_{ann} = 360^\circ\text{C}$, the GMR, Δ , and $M_r(\infty)$ decrease rapidly with further increase of the annealing temperature. The rapid increase of H_c and H_r in Fig. 4 shows that the size of the Co particles is degraded by increasing T_{ann} due to the breaking of the larger grains into smaller ones. This type of behavior of the coercivity on the particles size is well known for fine particle systems. The CF increases and Δ decreases very rapidly as well, showing that there is a setup of demagnetizing interactions between Co clusters. These interactions tend to align the moments of the particles to form flux-closure loops, thus resulting in the decrease of $M_r(\infty)$, increasing the values (negative) of Δ , and widening the switching field distribution of the magnetizations (H_r increases more rapidly than H_c , leading to the increase of the CF). This can be seen in Fig. 5, where representative magnetization curves and dc demagnetization remanence curves for the samples with Cr buffer annealed at 340 and 450°C are plotted.

Another contribution to the decrease of the saturation remanence and the increase of the coercivities can be the transition from fcc to hcp Co, observed by van Alphen and de Jonge²⁸ for higher annealing temperatures.

Thus, annealing at temperature higher than 360°C causes the decrease in GMR for two reasons:

- (1) decrease of the size and change of the distances between the magnetic particles; and *mainly*
- (2) appearance of demagnetizing interparticle interactions: the random alignment of the magnetizations of the mag-

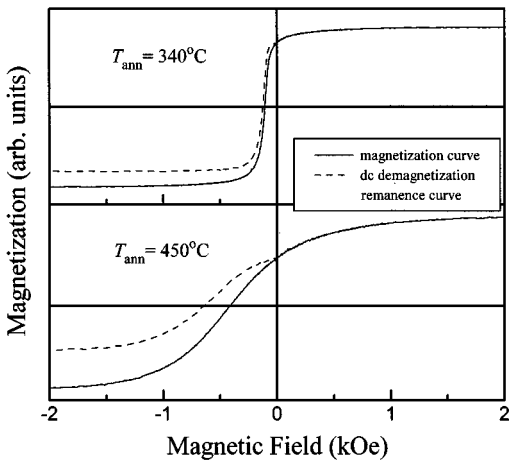


FIG. 5. Representative magnetization and dc demagnetization remanence curves for the sample with Cr buffer annealed at 340 °C and 450 °C.

netic precipitates is lost in a length scale larger than the mean free path of the conducting electrons.

It worth noting that GMR reaches its maximum for the same annealing temperature, where the magnetic interactions are minima: Δ , $M_r(\infty)$, and CF have values very close to the theoretical ones for a noninteracting fine particle system with cubic anisotropy.

In Fig. 6, the dependencies of GMR, Δ and $M_r(\infty)$ on T_{ann} for the sample without a Cr buffer layer are plotted. The dashed lines correspond to the annealing temperature range where planar magnetic anisotropy still exists, and the experimental points show the corresponding averaged values. It can be seen that for T_{ann} higher than 300 °C the shape of the

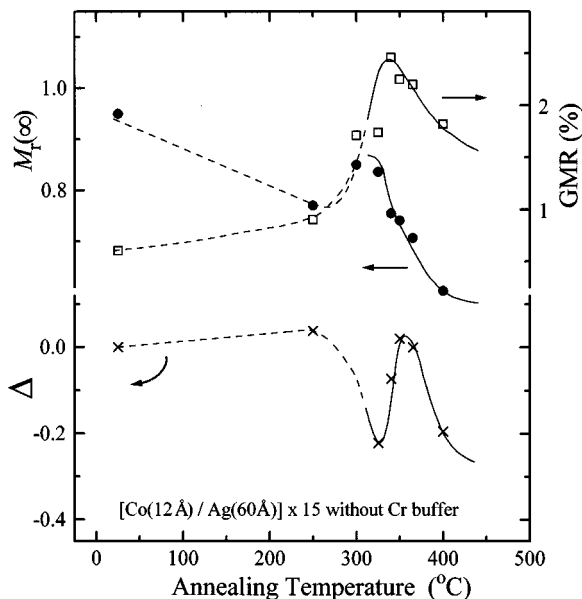


FIG. 6. GMR, Δ and the reduced saturation remanence $M_r(\infty)$ as a function of the annealing temperature for $[\text{Co}(12 \text{ \AA})/\text{Ag}(60 \text{ \AA})] \times 15$ multilayer without Cr buffer layer. The lines are guide to the eye, as the dashed lines correspond to the annealing temperature range where planar magnetic anisotropy still exists.

curves is the same as for the sample evaporated over the Cr buffer layer, which supports the discussion above.

V. CONCLUSION

The dependencies of the GMR, magnetization, and remanence curves on the annealing temperature in CoAg multilayered/granular systems have been examined. They have been explained as a result of the structural and magnetic evolution of the samples during annealing. For the lower annealing temperatures the increase of the GMR comes from the misalignment of the magnetic moments of the Co particles formed during the annealing. A strong correlation between the GMR and the magnetic interaction effects has been found for samples annealed at temperatures higher than 360 °C: GMR is degraded as a result of the increased demagnetizing interactions between the particles.

ACKNOWLEDGMENTS

This work has been supported by Conselho Nacional de Desenvolvimento Científico e Tecnológico (CNPq, Brazil), Fundação de Amparo à Pesquisa do Estado do Rio Grande do Sul (FAPERGS, Brazil), and Financiadora de Estudos e Projetos (FINEP, Brazil).

- ¹M. N. Baibich, J. M. Broto, A. Fert, F. Nguyen Van Dau, F. Petroff, P. Etienne, G. Creuzet, A. Friederich, and J. Chazelas, *Phys. Lett. B* **61**, 2472 (1988).
- ²A. E. Berkowitz, A. P. Young, J. R. Mitchell, S. Zhang, M. J. Carey, F. E. Spada, F. T. Parker, A. Hutten, and G. Thomas, *Phys. Rev. Lett.* **68**, 3745 (1992).
- ³Q. Xiao, J. S. Jiang, and C. L. Chien, *Phys. Rev. Lett.* **68**, 3749 (1992).
- ⁴L. F. Schlep, G. Tosin, M. Carara, M. N. Baibich, A. A. Gomes, and J. E. Schmidt, *Appl. Phys. Lett.* **61**, 1858 (1992).
- ⁵G. Tosin, L. F. Schelp, M. Carara, J. E. Schmidt, A. A. Gomes, and M. N. Baibich, *J. Magn. Magn. Mater.* **121**, 399 (1993).
- ⁶T. L. Hylton, K. R. Coffey, M. A. Parker, and J. K. Howard, *Science* **261**, 1021 (1993).
- ⁷B. J. Hickey, M. A. Howson, S. O. Musa, and N. Wisser, *Phys. Rev. B* **51**, 667 (1995).
- ⁸J. F. Gregg, S. M. Thompson, S. J. Dawson, K. Ounadjela, C. R. Staddon, J. Hamman, C. Fermon, G. Saux, and K. O'Grady, *Phys. Rev. B* **49**, 1064 (1994).
- ⁹M. El-Hilo, K. O'Grady, and R. W. Chantrell, *J. Appl. Phys.* **76**, 6811 (1994).
- ¹⁰P. Allia, M. Knobel, P. Tiberto, and F. Vinai, *Phys. Rev. B* **52**, 15398 (1995).
- ¹¹C. Bellouard, B. George, and G. Marchal, *J. Phys., Condens. Matter.* **6**, 7239 (1994).
- ¹²H. J. Blythe and V. M. Fedosyuk, *J. Phys., Condens. Matter.* **7**, 3461 (1995).
- ¹³A. Gavrin, M. H. Kelley, J. Q. Xiao, and C. L. Chien, *Appl. Phys. Lett.* **66**, 1683 (1995).
- ¹⁴P. E. Kelly, K. O'Grady, P. I. Mayo, and R. W. Chantrell, *IEEE Trans. Magn.* **25**, 3881 (1989).
- ¹⁵M. R. Parker, D. Seale, E. Tsang, J. A. Barnard, S. Hossain, D. A. Richards, and M. L. Watson, *J. Appl. Phys.* **73**, 6408 (1993).
- ¹⁶A. D. C. Viegas, J. Geshev, L. S. Dorneles, J. E. Schmidt, and M. Knobel (unpublished).
- ¹⁷E. P. Wohlfarth, *J. Appl. Phys.* **29**, 595 (1958).
- ¹⁸O. Henkel, *Phys. Status Solidi* **7**, 919 (1964).
- ¹⁹R. A. McCurie and P. Gaunt, *Proceedings of the International Conference on Magnetism, Nottingham, 1964*, p. 780.
- ²⁰M. Fearon, R. W. Chantrell, and E. P. Wohlfarth, *J. Magn. Magn. Mater.* **86**, 197 (1990).
- ²¹P. Bissel, R. Chantrell, G. Tomka, J. Knowles, and M. Sharrock, *IEEE Trans. Magn.* **25**, 3650 (1989).
- ²²R. Gans, *Ann. Phys. Leipzig* **15**, 28 (1932).

- ²³J. Geshev and M. Mikhov, *J. Magn. Magn. Mater.* **104–107**, 1569 (1992).
- ²⁴P. I. Mayo, K. O'Grady, P. E. Kelly, J. Cambridge, I. L. Sanders, T. Yogi, and R. W. Chantrell, *J. Appl. Phys.* **69**, 4733 (1991).
- ²⁵X. Che and H. N. Bertram, *J. Magn. Magn. Mater.* **116**, 121 (1992).
- ²⁶I. A. Al-Omari and D. J. Sellmyer, *Phys. Rev. B* **52**, 3441 (1995).
- ²⁷S. Duan, R. Khan, S. Y. Lee, L. Pressesky, L. Tang, and G. Thomas, *IEEE Trans. Magn.* **27**, 5055 (1991).
- ²⁸E. A. M. van Alphen and W. J. M. de Jonge, *Phys. Rev. B* **51**, 8182 (1995).
- ²⁹E. A. M. van Alphen, P. A. A. van der Heijden, and W. J. M. de Jonge, *J. Magn. Magn. Mater.* **140–144**, 609 (1995).
- ³⁰A. R. Corradi and E. P. Wohlfarth, *IEEE Trans. Magn.* **14**, 861 (1978).
- ³¹D. Altbir, J. d.'Albuquerque e Castro, and P. Vargas, *Phys. Rev. B* **54**, 6823 (1996).